THE ENZYMES

Molecular Machines Involved in Protein Transport across Cellular Membranes

Edited by
Ross E. Dalbey
Carla M. Koehler
Fuyuhiko Tamanoi

VOLUME XXV

THE ENZYMES

Edited by

Ross E. Dalbey

Department of Chemistry
The Ohio State University
Columbus, OH 43210, USA

Carla M. Koehler

Department of Chemistry and Biochemistry
University of California, Los Angeles
Los Angeles, CA 90095, USA

Fuyuhiko Tamanoi

Department of Microbiology, Immunology, and Molecular Genetics
Molecular Biology Institute
University of California, Los Angeles
Los Angeles, CA 90095, USA

Volume XXV

MOLECULAR MACHINES INVOLVED IN PROTEIN TRANSPORT ACROSS CELLULAR MEMBRANES

ELSEVIER

AMSTERDAM • BOSTON • HEIDELBERG • LONDON
NEW YORK • OXFORD • PARIS • SAN DIEGO
SAN FRANCISCO • SINGAPORE • SYDNEY • TOKYO
Academic Press is an imprint of Elsevier

Academic Press is an imprint of Elsevier
84 Theobald's Road, London WC1X 8RR, UK
Radarweg 29, PO Box 211, 1000 AE Amsterdam, The Netherlands
Linacre House, Jordan Hill, Oxford OX2 8DP, UK
30 Corporate Drive, Suite 400, Burlington, MA 01803, USA
525 B Street, Suite 1900, San Diego, CA 92101-4495, USA

First edition 2007

ISBN: 978-0-12-373916-2
ISSN: 1874-6047

For information on all Academic Press publications visit our website at books.elsevier.com

Printed and bound in USA

07 08 09 10 11 10 9 8 7 6 5 4 3 2 1

The Enzymes

VOLUME XXV

MOLECULAR MACHINES INVOLVED IN PROTEIN TRANSPORT ACROSS CELLULAR MEMBRANES

Preface

Proteins are synthesized in the cytosol but need to be transported to proper cellular locations for their action. How this intracellular transport is accomplished is one of the central issues in biology. We now know that this process involves targeting sequences on the protein as well as machines (multiprotein complexes) in the membrane that facilitate transport of proteins across cellular membranes. Recently, we have seen dramatic advances in our understanding of various machines involved in protein transport across cellular membranes in prokaryotes and eukaryotes. This volume is intended to bring together a diverse range of study involving molecular machines for protein transport across membranes. While previous publications dealt more with targeting signals on the protein or biogenesis of organelles, we tried to focus our attention on the machines that operate to facilitate uptake of proteins across the membrane. Our hope is that the volume will convey wealth of knowledge on diverse machines that function in various cellular membranes to facilitate protein transport. Similarities and differences of these systems are discussed.

Chapters are grouped into five different sections. Part I focuses on bacterial membranes. First, machines involved in the membrane targeting and transport through the inner membrane such as SRP, Sec, YidC, and Tat are discussed. This is followed by the discussion on the machines in the outer membrane. Protein transport into endoplasmic reticulum is discussed in Part II. Topics in this section cover SRP and Sec as well as chaperones such as BiP/ker2p and ERp57. Part III deals with the transport of proteins into mitochondria and describes inner membrane and outer membrane machines. TOM and SAM complexes as well as TIM complex are discussed. Part IV describes protein transport into chloroplast in plants. TOC and TIC complexes operate at the outer and inner envelope of chloroplast, respectively. In addition, Sec and TAT pathways function to transport proteins across the thylakoid membrane into the lumen. In the final section (Part V), we discuss mechanisms of peroxisomal protein import.

Because unfolding is one of the important features of protein transport process, two chapters (Chapters 5 and 13) discuss the significance of disulfide bond formation. In addition, some chapters include discussions on the comparison of the Sec pathway that transports substrates in an unfolded

state and the Tat pathway that transports substrates in a folded state. It is also important to point out that similar transport mechanisms operate in different systems. For example, SRP and Sec complexes are used in bacterial systems as well as in the import into endoplasmic reticulum of eukaryotic systems. The Tat machinery is present in bacterial systems as well as in chloroplasts in plants. Chapters 3 and 18 contain discussions on this conservation of transport machines and discussion on how studies in bacterial and plant systems facilitated our understanding of this transport machine.

The idea for this volume was conceived by one of us (R.D.). We have been able to bring this initial idea to publication in a short period of time. This is in large part due to the effort of the contributors to prepare their chapters in a timely fashion. We would like to thank the authors for making this publication a reality. We also thank Tari Broderick and Renske van Dijk for their expert help in the preparation of this volume.

Fuyuhiko Tamanoi
Ross Dalbey
Carla Koehler
April 20, 2007

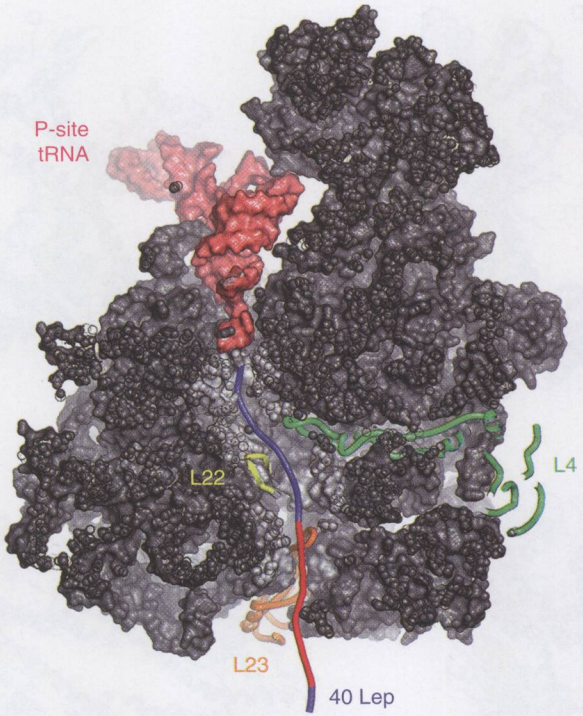

RONALD S. ULLERS *ET AL.*, FIG. 1.1, PAGE 7. The molecular environment of 40Lep in the ribosomal tunnel. The 40 amino acid residues nascent Leader Peptidase [Lep] (blue) and TM segment (red) is stretched from P-site tRNA (salmon pink) to the ribosomal exit site, and makes contact in the tunnel with ribosomal proteins L22 (yellow), L4 (green), and L23 (orange). (*Reprinted from* The Journal of Cell Biology *[17].*)

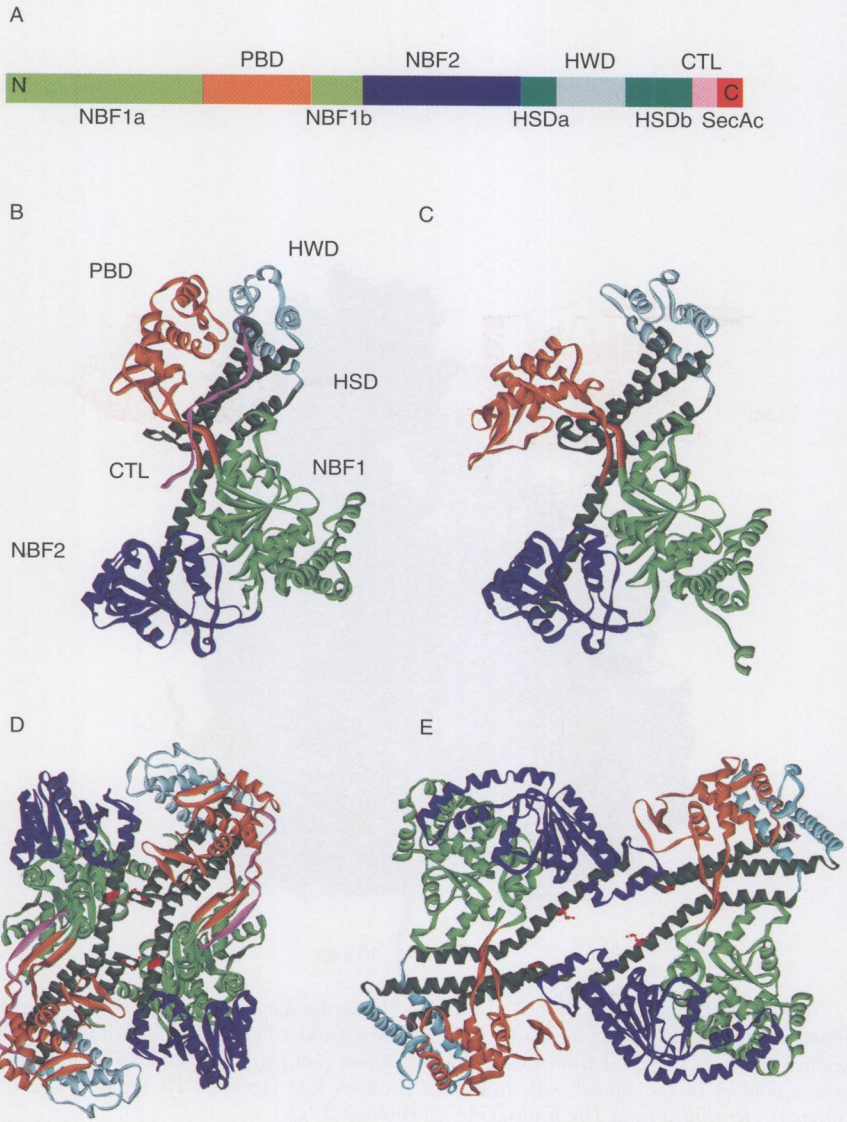

ELI O. VAN DER SLUIS *ET AL.*, FIG. 2.3, PAGE 44. Structure of SecA. (A) Schematic overview of the domain structure of SecA. NBF: nucleotide-binding fold; PBD: preprotein-binding domain; HSD: helical scaffold domain; HWD: helical wing domain; CTL: C-terminal linker; SecAc: SecB-binding motif. (B) Crystal structure of SecA protomer from *B. subtilis* with individual domains colored as in (A) [13]. (C) Crystal structure of SecA from *B. subtilis* in an open conformation, possibly representing the (pre)protein-bound state [75]. The conformational changes with respect to the structure depicted in (B) are indicated by arrows. (D) Crystal structure of dimeric SecA from *B. subtilis* that most likely represents the physiologically active dimer [13]. The two intradimeric HSD–HSD contacts that are maintained during protein translocation are depicted in red [95]. (E) Crystal structure of *M. tuberculosis* SecA.

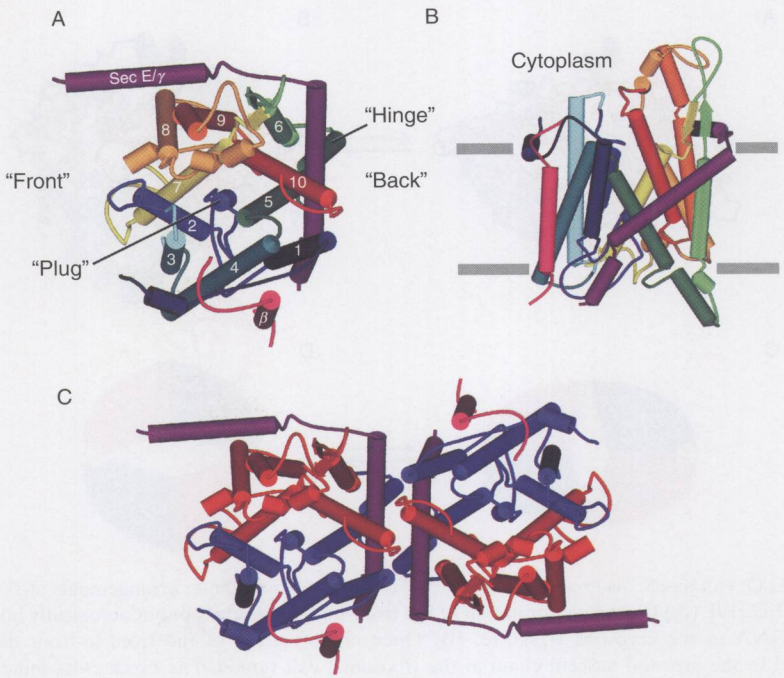

ELI O. VAN DER SLUIS *ET AL.*, FIG. 2.5, PAGE 52. Structure of SecYEβ from *M. jannaschii* [16]. (A) Cytoplasmic view showing the arrangement of transmembrane segments in different colors. SecE is depicted in purple, Secβ in pink. Sides referred to as "front" and "back" are indicated. (B) View from within the plane of the membrane showing the two cytoplasmic loops that extend into the cytoplasm and have been shown to interact with the ribosome and SecA: C4 and C5, connecting TMS6 with TMS7 and TMS8 with TMS9, respectively. (C) Back-to-back dimer arrangement of SecYEβ protomers as observed for *E. coli* SecYEG in two-dimensional crystals [118]. The N-terminal halves of SecY are depicted in blue, the C-terminal halves in red, and SecE and Secβ in purple and pink, respectively.

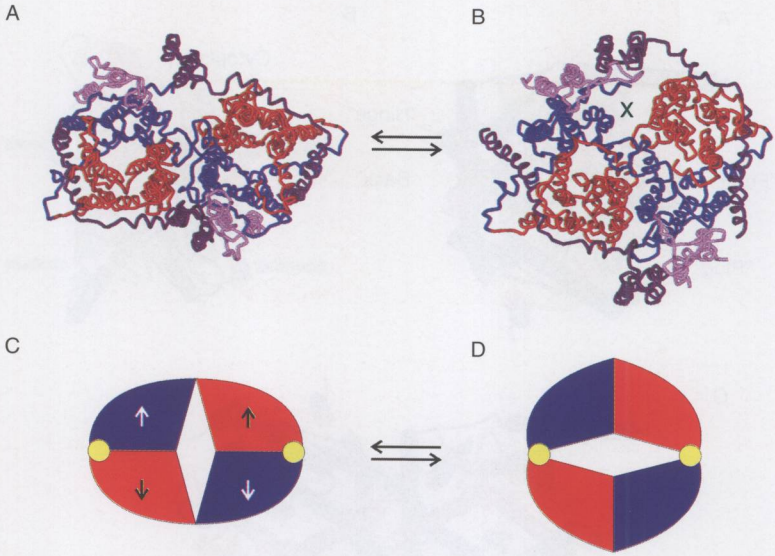

ELI O. VAN DER SLUIS *ET AL.*, FIG. 2.6, PAGE 57. Front-to-front dimer arrangements of *E. coli* SecYEG [19]. (A) Closed conformation of the front-to-front dimer, nonphysiologically bound to mRNA in the cryo-EM structure. (B) Open conformation of the front-to-front dimer bound to the arrested nascent chain at the ribosomal exit tunnel. The black cross indicates the position of the electron density that possibly corresponds to the arrested nascent chain. In (A) and (B), the N-terminal halves of SecY are depicted in blue, the C-terminal halves in red, SecE in pink, and SecG in green. (C) and (D) Schematic representation of the proposed ribosome/SecA-induced opening mechanism. A simultaneous interaction of the ribosome or SecA with the N-terminal (blue) and C-terminal (red) domain of one or two SecY molecules could induce opening of the translocon via outward directed forces. The proposed hinge region (loop E3 connecting TMS5 and TMS6) is represented by yellow circles, the proposed outward directed forces are indicated by arrows. The large clefts within both states of the translocon are merely for illustrative purposes.

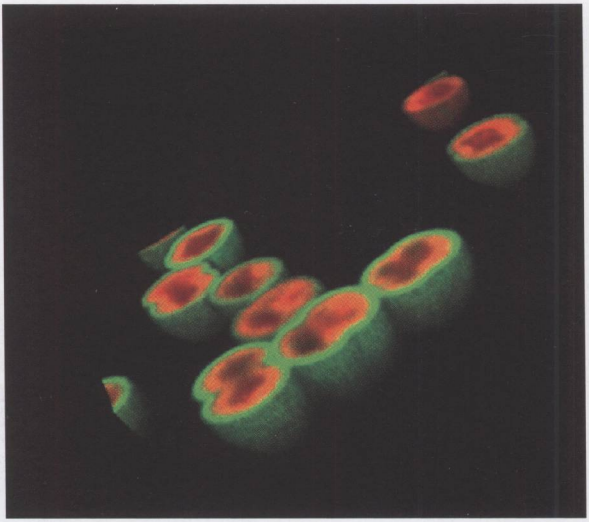

SHARON MENDEL AND COLIN ROBINSON, FIG. 3.2, PAGE 75. Export of a heterologous protein, GFP, by the Tat pathway in cyanobacteria. The image shows a *Synechocystis* PCC6803 transformant expressing a construct comprising a Tat signal peptide (from *E. coli* TorA) linked to GFP. The cells were analyzed by confocal microscopy followed by 3D rendering, and the periplasmic GFP is visible as a green halo surrounding the internal thylakoids (which emit red fluorescence). Image courtesy of Anja Nenninger.

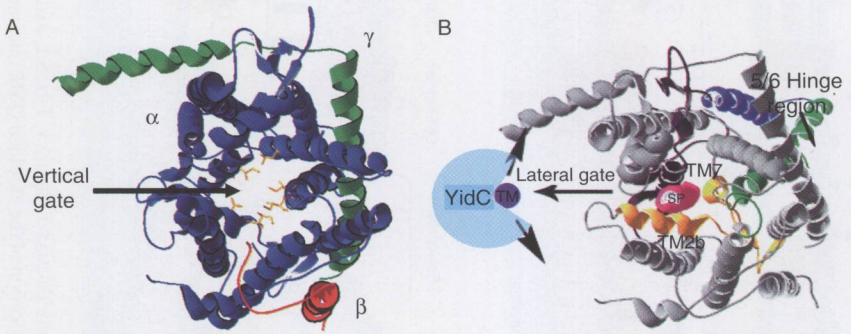

NIL CELEBI AND ROSS E. DALBEY, FIG. 4.2, PAGE 98. Structure of the *M. janashii* Sec61αβγ. (A) Protein fold of Sec61αβγ showing the pore residues (view from the cytosol). Sec61α is shown in blue, Sec61γ in green, Sec61β in red, the six hydrophobic residues lining the pore ring are shown in yellow. Note that the plug is removed. (B) Putative lateral gate (TM2b/TM7) interface region (view from the cytosol). Sec61α TM5 and TM6 are indicated in green and blue, respectively. The hinge region between these transmembrane segments is indicated. TM2 is indicated in yellow and TM7 in purple. The hydrophobic core of the signal peptide (SP) is indicated in pink. SP is intercalated between TM2b and part of TM7. *Modified from* Nature *[4] with permission.*

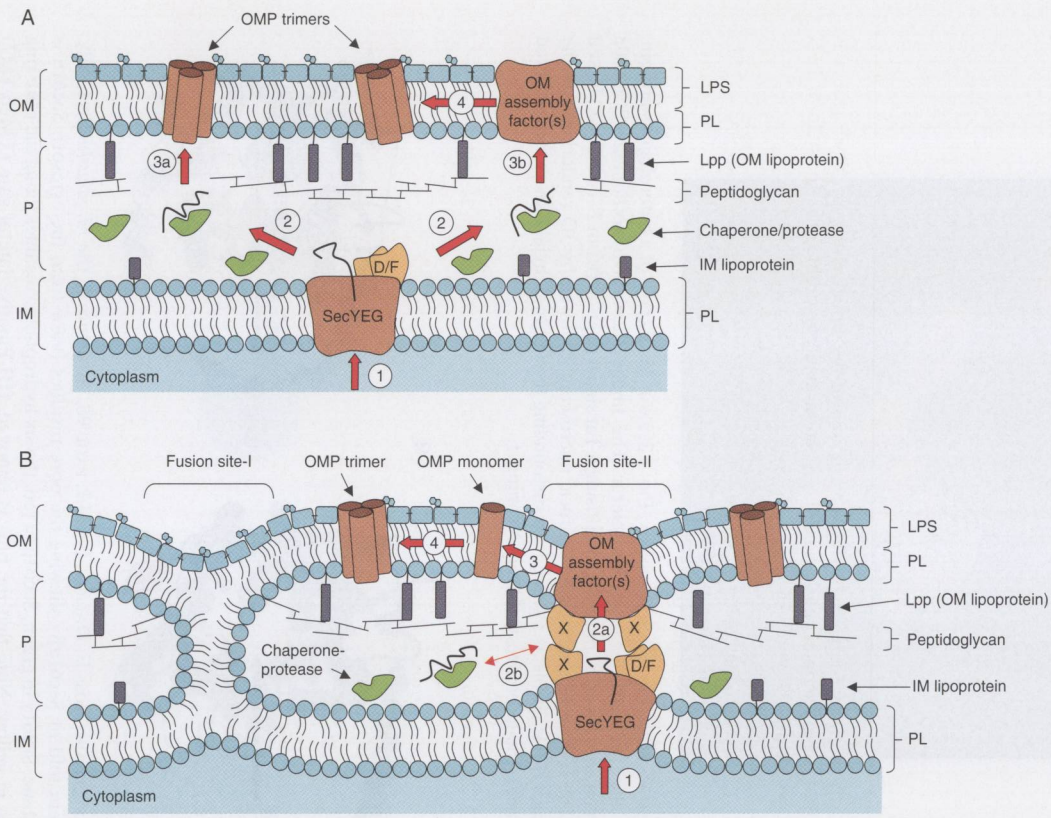

JULIANA MALINVERNI AND THOMAS J. SILHAVY, FIG. 6.1, PAGE 132. Transport models across and into bacterial membranes. (A) Periplasmic intermediate model. Translocation of the unfolded OMP intermediate (shown as a bold black line) occurs through the SecYEG translocon (step 1). SecD and SecF (labeled D/F in the sketch) appear to facilitate translocation and/or release of OMPs from the IM [2]. Subsequent to the processing of the signal sequence, the unfolded mature protein binds to a periplasmic chaperone such as Skp or SurA, which ferries the intermediate from the

IM across the periplasm (step 2) [9]. Some variations of the model assert that OMP assembly into the OM occurs spontaneously, and the reaction made favorable with the help of LPS, phospholipid, and/or interactions with the periplasmic chaperone foldases (step 3a). Alternatively, the periplasmic chaperones deliver the OMP substrate to an OM assembly site (step 3b). This assembly machine may either indirectly catalyze the OMP insertion reaction by providing localized chaperone activity near the inner leaflet of the OM, or it may constitute a translocon analogous to the IM Sec/SRP pathway that requires transport of OMP substrate through a porin chamber followed by lateral release of folded mature protein (steps 3b and 4) [2]. (B) Bayer's Patch Model. This model evokes putative contact sites between the IM and OM [11]. Although these sites may be lipid in nature (as shown in fusion site – I), we favor the hypothesis that contact sites would most likely be proteinaceous in nature (as shown in fusion site – II). In this model, the Sec translocon transiently docks to the OM assembly machinery. Transport of the OMP precursor across the IM occurs as described above and in the text (step 1). Mature unfolded OMP substrates then cross the periplasmic barrier through a proteinaceous channel composed of unknown proteins (depicted as "X" in the sketch) (step 2a). At this point, it is conceivable that OMPs could escape the "transport tunnel" into the periplasmic space on saturation of the assembly pathway, where they are solubilized by periplasmic chaperones (step 2b). Successful translocation events across the protein channel would result in the recognition of the unfolded OMP by OM assembly factor(s) and subsequent assembly into the OM (step 3). The process by which this may occur is unknown (see text). (A and B) Many proteins exist in a trimeric state in the OM, and it is unknown how this association is initiated. It may be that trimerization of monomeric subunits is catalyzed by a series of monomer–lipid interactions, or it may be that an additional OM assembly factor is required for multimerization (trimerization depicted in panel B, step 4).

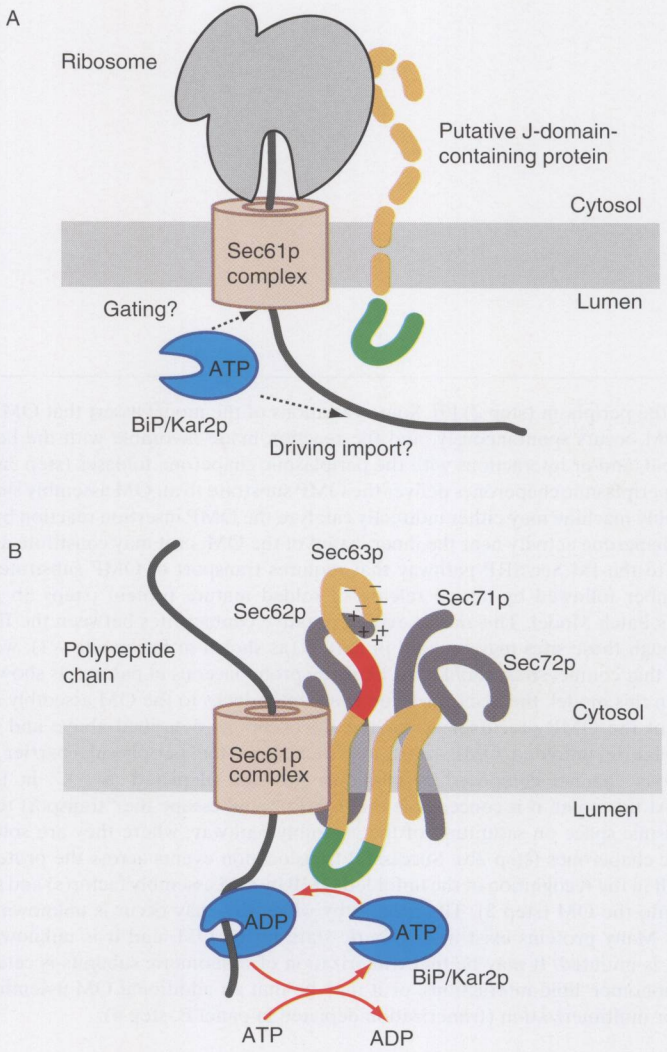

KUNIO NAKATSUKASA AND JEFFREY L. BRODSKY, FIG. 10.2, PAGE 252. (A) During cotranslational translocation, translation and translocation are coupled. Polypeptide chains are synthesized by the ER-bound ribosome and are transported into the ER lumen through the Sec61p complex, which includes Sec61p, Sbh1p, and Sss1p in yeast. The ER lumenal chaperone, BiP/Kar2p, may facilitate import by binding to the substrate. BiP/Kar2p may also seal the lumenal end of the translocon to prevent the passage of small molecules. Some J-domain-containing proteins (the J-domain is indicated in green) are proposed to function in these processes (see text for details). (B) During posttranslational translocation, translation and translocation are uncoupled. The ATPase activity of BiP/Kar2p is stimulated by the J-domain in Sec63p (the J-domain is indicated in green). BiP/Kar2p binds to the polypeptide chain emerging from the Sec61p complex and facilitates translocation. The acidic domain at the C-terminus of Sec63p interacts with the C-terminus of Sec62p. The Brl domain in Sec63p (red region) is required to assemble a multiprotein complex that along with BiP is sufficient for translocation *in vitro* [97] and that contains the Sec61p, Sec62p, Sec63p, Sec71p, and Sec72p complexes [103].

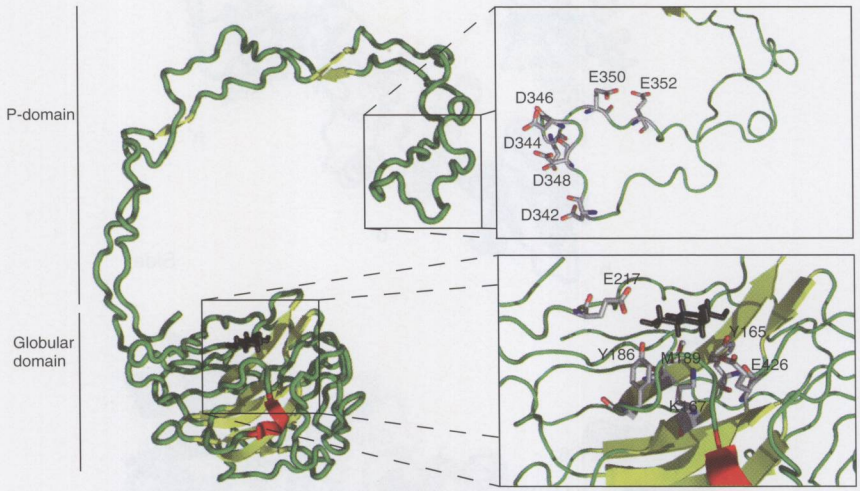

BRADLEY R. PEARSE AND DANIEL N. HEBERT, FIG. 11.3, PAGE 279. Crystal structure of soluble calnexin and insight into the lectin and ERp57-docking sites. The 2.9-Å crystal structure of soluble canine calnexin (PDB code: 1JHN) is colored by structural elements with β-strands in yellow, α-helices in red, and unstructured loops in green. The general boundaries of the P-domain and the globular domain are indicated with bars. The site of ERp57 docking on the tip of the P-domain is enlarged to display residues that are important for the interaction [19]. Also enlarged is the lectin-binding site with the residues that coordinate the bound glucose highlighted [10]. A hypothetical positioning of glucose is included to emphasize where the oligosaccharide is bound. Labeled residues are colored by elements. Molecular graphics were created using the PYMOL program.

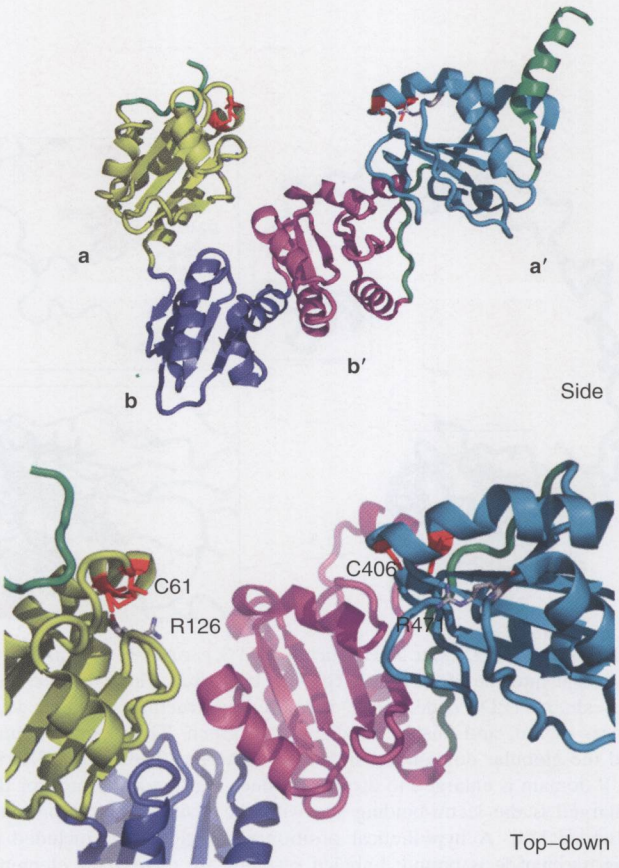

Bradley R. Pearse and Daniel N. Hebert, Fig. 11.7, page 291. Crystal structure of yeast PDI. The 2.4-Å crystal structure of yeast PDI is depicted in both a side view and a top view (PDB code: 2B5E). The thioredoxin domains **a, b, b′**, and **a′** are colored yellow, blue, purple, and cyan, respectively. Active site Cys residues are colored red and the conserved Arg residue is colored by element, both are represented in stick form and labeled accordingly.

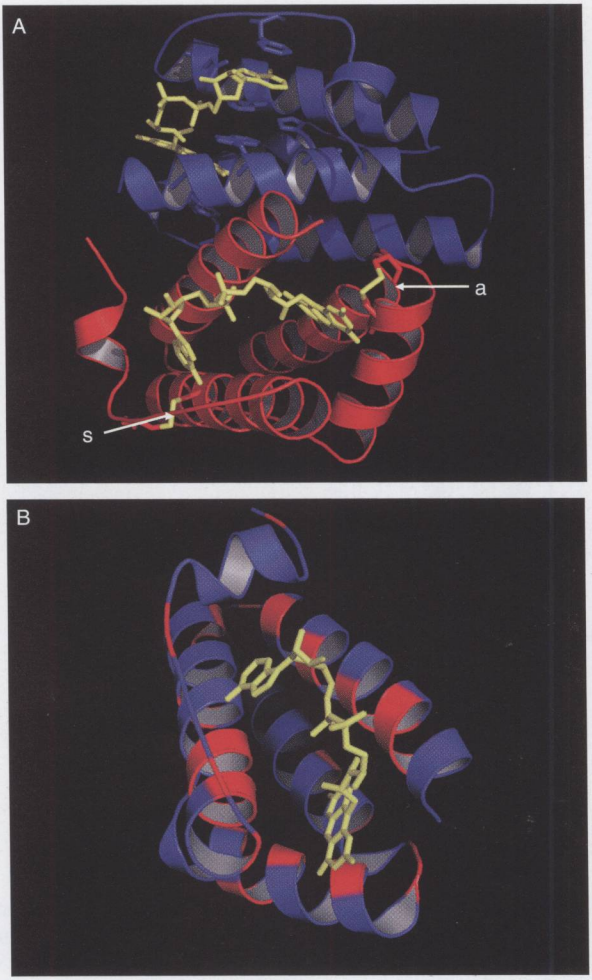

JOHANNES M. HERRMANN *ET AL.*, FIG. 13.4, PAGE 354. Comparison of the molecular structures of Erv1 and Erv2. A colored version of this figure is displayed at the end of this volume. (A) Shown is a model of the molecular structure of the FAD-binding domains of an Erv1–Erv1 homodimer generated using the PyMOL software by molecular replacement on the basis of the PDB file 1JRA of Erv2 [36]. The FAD cofactors are shown in light gray (yellow in the colored version). Note that different structural details are indicated in the upper and lower subunit, which *in vivo* are identical. In the upper subunit (shown in blue in the colored version), the aromatic side chains that fix the FAD group via hydrophobic stacking interactions are illustrated. In the lower subunit (shown in red in the colored version), the two disulfide bridges in the FAD-binding domain are depicted in light gray (or yellow, respectively). The redox-active disulfide bridge (indicated by a) is in direct proximity to the isoalloxazine group of FAD and exposed to the surface of Erv1. The structural disulfide bridge (indicated by s) fixes a flexible unstructured C-terminus of Erv1 to the α-helix that is close to the adenine group of the FAD molecule. (B) Enlarged view of the FAD-binding pocket of Erv2 [36]. Residues shown in light gray (or red in the colored version) are identical between Erv1 and Erv2, whereas residues in dark gray (or blue, respectively) are different. This illustrates that the side chains that contribute to the binding of FAD are practically identical between Erv1 and Erv2.